한국전산구조공학회
1996년도 봄학술발표회 논문집

후처리 에러산정을 위한 가상해 도출방법
Solution Recovery Techniques for Posteriori Error Estimation

이 상호* 김 상효**
Lee, Sang-Ho Kim, Sang-Hyo

ABSTRACT

An enhanced solution recovery method for recovering accurate derivatives such as moments, or shears, from finite element solutions for C^0 beam and plate is presented. In the enhanced method, the square of the residuals in the equilibrium equations is included. Results are compared with those of standard Zienkiewicz-Zhu methods. Numerical examples show that in the global projection, the enhanced technique improves the accuracy of projected solution significantly. In the local projection, the enhanced method circumvents the numerical ill-conditioning which occurs in some meshes, and usually recovers derivatives with better accuracy.

1. INTRODUCTION

Several investigators have recently reported the use of adaptive techniques for plate problems. Zienkiewicz and Zhu(1989) used a least square fit of a C^0 interpolant to the finite element solution, which is often called L_2 projection, to devise an error measure. Meissner and Wibbeler(1991) have used bubble modes to develop error criteria. In general, the adaptive mesh refinement is dependent on a *posteriori* error estimation. The most popular solution recovering techniques for a *posteriori* error estimators are global and local projection methods.

The global projection method for obtaining a continuous solution originated from Hinton and Campbell(1974). It was applied by Zienkiewicz and Zhu to plane problems(1987) and plate bending problems(1989). This technique has been used frequently for the mesh adaptivity of plate and shell problems due to the simplicity of its implementation and its reasonable accuracy. The global projection is quite effective but has the following drawbacks: Recovery procedures are expensive with a consistent matrix and the use of a

* 연세대학교 토목공학과 조교수
** 연세대학교 토목공학과 부교수

lumped matrix decreases the accuracy of recovered solution; The recovered solution shows poor accuracy near the boundaries.

The local projection, unlike the global projection, uses the information of a local region to recover a continuous solution. Recently, a very effective local projection technique has been developed by Zienkiewicz and Zhu(1992). In this technique, a small patch of elements is used to recover the smoothed solution. The projected nodal derivatives in a patch can be obtained by a least square fit of a polynomial to the values of the superconvergent points of the patch. In general, this method is faster and often more accurate than the global projection. However, it was found that numerical singularities (or ill-conditioning) are encountered in certain element configurations which occur quite often in standard meshes.

In this paper, global and local projections with equilibrium residuals are developed. The addition of the equilibrium residual dramatically improves the performance of the global projection and circumvents the singularity in the local projection at almost no cost.

2. SOLUTION RECOVERY PROCEDURES

Enhanced Global Projection

In the enhanced least square form for global projection, the equilibrium residual is added to the standard least square term of Mindlin-Reissner plate, so

$$\Pi_G = \alpha_1 \int_\Omega (\mathbf{m}^* - \mathbf{m}^h)^T (\mathbf{m}^* - \mathbf{m}^h)\, d\Omega + \alpha_2 \int_\Omega (\mathcal{D}_1^T \mathbf{m}^* - \mathbf{q}^h)^T (\mathcal{D}_1^T \mathbf{m}^* - \mathbf{q}^h)\, d\Omega$$
$$+ \alpha_1 \int_\Omega (\mathbf{q}^* - \mathbf{q}^h)^T (\mathbf{q}^* - \mathbf{q}^h)\, d\Omega + \alpha_2 \int_\Omega (\mathcal{D}_2^T \mathbf{q}^* + p)^T (\mathcal{D}_2^T \mathbf{q}^* + p)\, d\Omega \qquad (1)$$

where $\mathbf{m}^*$ and $\mathbf{q}^*$ are the projected moment and shear, respectively, and $\mathbf{m}^h$ and $\mathbf{q}^h$ are C^{-1} finite element solutions. $\mathcal{D}_1$ and $\mathcal{D}_2$ are differential operators between moments and transverse shears, and transverse shears and distributed load. The parameters α_1 and α_2 are relative weightings which are usually set to 1.0 in this study. The terms related to the weighting α_2 are the residuals in the equilibrium equations.

The projected moments and shears are expressed in terms of continuous shape functions $\mathbf{N}(\mathbf{x})$ and nodal parameters $\overline{\mathbf{m}}^*$ and $\overline{\mathbf{q}}^*$, so

$$\mathbf{m}^*(\mathbf{x}) = \mathbf{N}_m(\mathbf{x})\, \overline{\mathbf{m}}^*, \qquad \mathbf{q}^*(\mathbf{x}) = \mathbf{N}_q(\mathbf{x})\, \overline{\mathbf{q}}^* \qquad (2)$$

$$\mathcal{D}_1^T \mathbf{m}^*(\mathbf{x}) = \mathcal{D}_1^T \mathbf{N}_m(\mathbf{x})\, \overline{\mathbf{m}}^*, \qquad \mathcal{D}_2^T \mathbf{q}^*(\mathbf{x}) = \mathcal{D}_2^T \mathbf{N}_q(\mathbf{x})\, \overline{\mathbf{q}}^* \qquad (3)$$

where $\mathbf{N}_m$ and $\mathbf{N}_q$ are block diagonal matrices of the shape functions $\mathbf{N}$ for the moments and shears. The shape functions $\mathbf{N}$ are usually taken to be of the same order as used for the finite element displacement field.

Substituting equations (2) and (3) into (1) and then minimizing (1) with respect to the unknown nodal parameters $\overline{\mathbf{m}}^*$ and $\overline{\mathbf{q}}^*$ gives the global equations (4).

$$\int_\Omega \begin{bmatrix} \alpha_1 \mathbf{N}^T\mathbf{N} + \alpha_2 \mathbf{N}_{,x}^T\mathbf{N}_{,x} & 0 & \alpha_2 \mathbf{N}_{,x}^T\mathbf{N}_{,y} & 0 & 0 \\ 0 & \alpha_1 \mathbf{N}^T\mathbf{N} + \alpha_2 \mathbf{N}_{,y}^T\mathbf{N}_{,y} & \alpha_2 \mathbf{N}_{,y}^T\mathbf{N}_{,x} & 0 & 0 \\ \alpha_2 \mathbf{N}_{,y}^T\mathbf{N}_{,x} & \alpha_2 \mathbf{N}_{,x}^T\mathbf{N}_{,y} & \alpha_1 \mathbf{N}^T\mathbf{N} + \alpha_2(\mathbf{N}_{,x}^T\mathbf{N}_{,x} + \mathbf{N}_{,y}^T\mathbf{N}_{,y}) & 0 & 0 \\ 0 & 0 & 0 & \alpha_1 \mathbf{N}^T\mathbf{N} + \alpha_2 \mathbf{N}_{,x}^T\mathbf{N}_{,x} & \alpha_2 \mathbf{N}_{,x}^T\mathbf{N}_{,y} \\ 0 & 0 & 0 & \alpha_2 \mathbf{N}_{,y}^T\mathbf{N}_{,x} & \alpha_1 \mathbf{N}^T\mathbf{N} + \alpha_2 \mathbf{N}_{,y}^T\mathbf{N}_{,y} \end{bmatrix} d\Omega \begin{bmatrix} \overline{\mathbf{m}}_x^* \\ \overline{\mathbf{m}}_y^* \\ \overline{\mathbf{m}}_{xy}^* \\ \overline{\mathbf{q}}_x^* \\ \overline{\mathbf{q}}_y^* \end{bmatrix}$$

$$= \int_\Omega \begin{bmatrix} \alpha_1 \mathbf{N}^T \mathbf{m}_x^h + \alpha_2 \mathbf{N}_{,x}^T \mathbf{q}_x^h \\ \alpha_1 \mathbf{N}^T \mathbf{m}_y^h + \alpha_2 \mathbf{N}_{,y}^T \mathbf{q}_y^h \\ \alpha_1 \mathbf{N}^T \mathbf{m}_{xy}^h + \alpha_2 (\mathbf{N}_{,y}^T \mathbf{q}_x^h + \mathbf{N}_{,x}^T \mathbf{q}_y^h) \\ \alpha_1 \mathbf{N}^T \mathbf{q}_x^h - \alpha_2 \mathbf{N}_{,x}^T \mathbf{p} \\ \alpha_1 \mathbf{N}^T \mathbf{q}_y^h - \alpha_2 \mathbf{N}_{,y}^T \mathbf{p} \end{bmatrix} d\Omega \,. \quad (4)$$

If the integral on the right hand side of (4) is evaluated assuming $\mathbf{m}^h$ and $\mathbf{q}^h$ are constant in each element, for example, taking $\mathbf{m}^h(\xi=\eta=0)$ and $\mathbf{q}^h(\xi=\eta=0)$ for four-node quadrilateral element, the accuracy of the recovered solutions is improved.

Enhanced Local Projection

In the local projection technique proposed by Zienkiewicz and Zhu(1992), the least square of the error is minimized over a small patch of elements. The function Π_L is evaluated by using a discrete set of the superconvergent points within that patch. The projected derivatives are assumed to be polynomials in the spatial variables as follows

$$\mathbf{m}^*(\mathbf{x}) = \mathbf{P}_m(\mathbf{x})\,\mathbf{a}_m\,, \qquad \mathbf{q}^*(\mathbf{x}) = \mathbf{P}_q(\mathbf{x})\,\mathbf{a}_q \quad (5)$$

where $\mathbf{P}_m$ and $\mathbf{P}_q$ are polynomial matrices defined as

$$\mathbf{P}_m = \begin{bmatrix} \mathbf{P} & 0 & 0 \\ 0 & \mathbf{P} & 0 \\ 0 & 0 & \mathbf{P} \end{bmatrix}, \qquad \mathbf{P}_q = \begin{bmatrix} \mathbf{P} & 0 \\ 0 & \mathbf{P} \end{bmatrix} \quad (6)$$

and the corresponding unknown coefficients $\mathbf{a}_m$ and $\mathbf{a}_q$ are

$$\mathbf{a}_m^T = \{\mathbf{a}_{mx}, \mathbf{a}_{my}, \mathbf{a}_{mxy}\}\,, \qquad \mathbf{a}_q^T = \{\mathbf{a}_{qx}, \mathbf{a}_{qy}\}\,. \quad (7)$$

In a four-node bilinear quadrilateral element, for instance,

$$\mathbf{P} = [1, x, y, xy], \qquad \mathbf{a}_{mx} = [a_1, a_2, a_3, a_4]^T_{mx}. \tag{8}$$

In the equilibrium enhanced local projection, the following is minimized for each patch:

$$\Pi_L = \alpha_1 \sum_{I=1}^{n} (\mathbf{m}^*(\mathbf{x}_I) - \mathbf{m}^h(\mathbf{x}_I))^2 + \alpha_2 \int_{\Omega_p} (\mathcal{D}_1{}^T \mathbf{m}^* - \mathbf{q}^h)^2 d\Omega$$
$$+ \alpha_1 \sum_{I=1}^{n} (\mathbf{q}^*(\mathbf{x}_I) - \mathbf{q}^h(\mathbf{x}_I))^2 + \alpha_2 \int_{\Omega_p} (\mathcal{D}_2{}^T \mathbf{q}^* + p)^2 d\Omega. \tag{9}$$

In equation (9), the summation of pointwise equilibrium residuals can also be used, but in general, the integration of the constraint condition over the whole patch improves the accuracy of the projection. Substituting (5) into (9), and minimizing it with respect to two sets of unknown coefficients $\mathbf{a}_m$ and $\mathbf{a}_q$ gives

$$[\alpha_1 \sum_{I=1}^{n} \mathbf{P}(\mathbf{x}_I)^T \mathbf{P}(\mathbf{x}_I) + \alpha_2 \int_{\Omega_p} (\mathcal{D}_1{}^T \mathbf{P})^T (\mathcal{D}_1{}^T \mathbf{P})] \mathbf{a}_m =$$
$$\alpha_1 \sum_{I=1}^{n} \mathbf{P}(\mathbf{x}_I)^T \mathbf{m}^h(\mathbf{x}_I) + \alpha_2 \int_{\Omega_p} (\mathcal{D}_1{}^T \mathbf{P})^T \mathbf{q}^h \, d\Omega \tag{10}$$

$$[\alpha_1 \sum_{I=1}^{n} \mathbf{P}(\mathbf{x}_I)^T \mathbf{P}(\mathbf{x}_I) + \alpha_2 \int_{\Omega_p} (\mathcal{D}_2{}^T \mathbf{P})^T (\mathcal{D}_2{}^T \mathbf{P})] \mathbf{a}_q =$$
$$\alpha_1 \sum_{I=1}^{n} \mathbf{P}(\mathbf{x}_I)^T \mathbf{q}^h(\mathbf{x}_I) - \alpha_2 \int_{\Omega_p} (\mathcal{D}_2{}^T \mathbf{P})^T p \, d\Omega \tag{11}$$

where n is the total number of superconvergent sampling points in the patch.

After solving (10) and (11), continuous nodal derivatives at any internal node J in the patch are obtained as follows:

$$\overline{\mathbf{m}}^*_J = \mathbf{P}_m(\mathbf{x}_J)\, \mathbf{a}_m, \qquad \overline{\mathbf{q}}^*_J = \mathbf{P}_q(\mathbf{x}_J)\, \mathbf{a}_q \tag{12}$$

3. NUMERICAL EXAMPLES

One Dimensional Examples

We used an inverse solution where cubic and quartic w functions are used to produce linear moment-constant transverse shear and quadratic moment-linear shear, respectively; see Table 1 for details. Uniform meshes (5, 10, 20, and 40 elements) are used for the finite element analyses.

The distribution of elemental estimated error measure $\|\mathbf{e}^*\|^2_e$ and exact error measure $\|\mathbf{e}^h\|^2_e$ are shown in Fig. 1. The legend "Exact" in Fig. 1 denotes $\|\mathbf{e}^h\|^2_e$. Convergence rates of the projection error, $\|\mathbf{e}^p\|$, are shown in Fig. 2. The results show that the enhanced method shows better accuracy in the evaluation of the estimated error, which is often used as error

indicator for mesh adaptivity. In the standard global projection method using a consistent matrix, the elemental projection error measure $\|\mathbf{e}^P\|_e^2$ is oscillatory. The results in Fig. 1 for the estimated error computed by the global projection using a lumped matrix appear to be quite accurate. However, the accuracy of the projection itself is quite poor as can be seen in Fig. 2.

Table 1 Beam solutions for the one dimensional patch models

	cubic w	quartic w
$w(x)$	$x^3 - 6rx$	$x^4 - 12rx^2$
$\theta(x)$	$3x^2$	$4x^3$
$m(x)$	$-6xD_m$	$-12x^2D_m$
$q(x)$	$-6D_m$	$-24xD_m$
$p(x)$	0	$24D_m$

where $D_m = EI$, $D_q = k_sGA$, and $r = D_m/D_q$.
$r = \dfrac{(1+\nu)t^2}{5}$ for homogeneous isotropic beam.
All variables are multiplied by a scaling factor to render them small and geometrically linear.

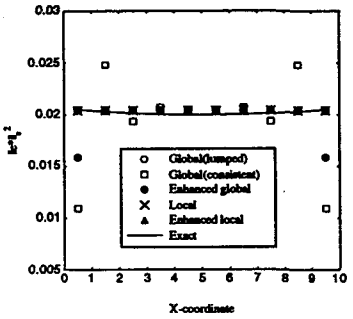

(a) Beam patch model with cubic w

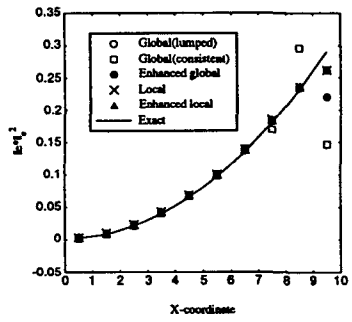

(b) Beam patch model with quartic w

Fig. 1 The distribution of elemental estimated errors ($\|e^*\|_e^2$) in 1-D beam models

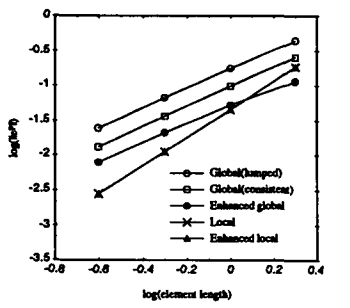

(a) Beam patch model with cubic w

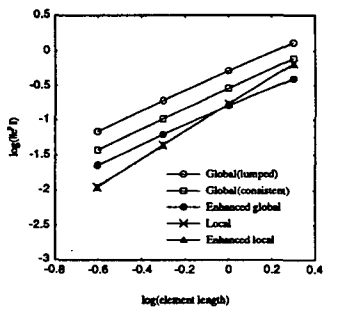

(b) Beam patch model with quartic w

Fig. 2 Convergence rates of the energy norms of projection errors ($\|e^P\|$) in 1-D beam models

Two Dimensional Plate Examples

The Wempner-Bathe-Dvorkin four-node shell element [Wempner, et al. (1982), and Dvorkin and Bathe(1984)] is used for the 2-D plate problems. This element is free from shear locking so full integration is used to compute the stiffness matrix. Fig. 3 and 4 show a clamped circular plate model with a uniform pressure load and a simply supported square plate subjected to a sinusoidal load, $p = p_o \sin \frac{\pi x}{a} \sin \frac{\pi y}{b}$.

Convergence rates of the energy norms of projection errors, $\|e^p\|$, in the clamped circular plate are shown in Fig. 5. This results show that the enhanced method shows better accuracy than the standard method. In Fig. 5, the accuracy of enhanced local projection is better than that of standard local projection method since in standard local projection, large error occur in some localized regions because of ill conditioning. Fig. 6 shows the convergence rates of $\|e^p\|$ in the square plate under sinusoidal load. In the coarsest mesh, the standard local projection shows better accuracy than the enhanced local projection. This may be explained by the poor discretization of the distributed load in the coarsest mesh. As the mesh is refined, the equilibrium enhanced local projection method becomes more accurate.

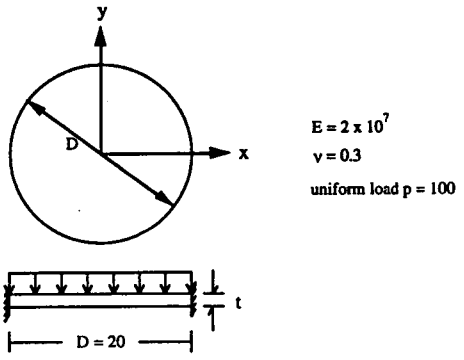

Fig. 3 Circular plate model

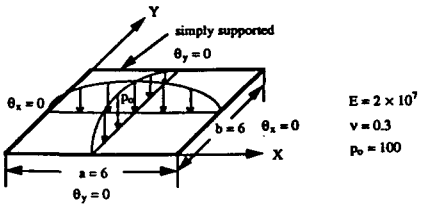

Fig. 4 Square plate model

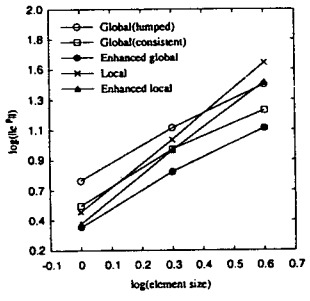

Fig. 5 Convergence rates of the energy norms of projection errors ($\|e^p\|$) for circular plate

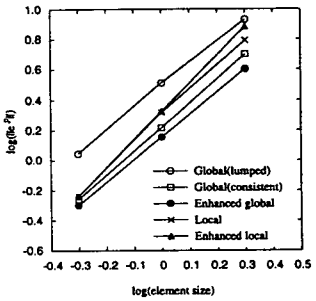

Fig. 6 Convergence rates of the energy norms of projection errors ($\|e^p\|$) for square plate

6. SUMM AND CONCLUSIONS

An enhanced solution recovery method which includes the squares of the residuals of the equilibrium equations has been described. This technique was applied in both global and local projection schemes for the C^0 beam and plate problems.

The equilibrium enhanced global and local projection methods show the following advantages:

1. The enhanced global projection method improves the accuracy of projected solutions significantly, especially near the boundaries.
2. The enhanced local projection method circumvents the ill-conditioning caused by certain frequently encountered element configurations and increases the accuracy of the recovered solutions.
3. It has been shown that these advantages hold for both thin and thick plates.

ACKNOWLEDGMENT

The support of Yonsei University is gratefully acknowledged.

REFERENCES

1. E. N. Dvorkin and K. J. Bathe, "A continuum mechanics based four-node shell element for general nonlinear analysis", *Eng. Comp.*, **1**, 77-88 (1984).
2. E. Hinton and J. Campbell, "Local and global smoothing of discontinuous finite element functions using a least square method", *Int. J. Numer. Meth. Eng.*, **8**, 461-480 (1974).
3. U. Meissner and H. Wibbeler, "A least square principle for the a posteriori computation of finite element approximation errors", *Comp. Meth. Appl. Mech. Eng.*, **85**, 89-108 (1991).
4. G. Wempner, D. Talaslidis and C.M. Hwang, "A simple and efficient approximation of shells via finite quadrilateral elements", *J. Appl. Mech. ASME*, **49**, 115-120 (1982).
5. O. C. Zienkiewicz and J. Z. Zhu, "A simple error estimator and adaptive procedure for practical engineering analysis", *Int. J. Numer. Meth. Eng.*, **24**, 337-357 (1987).
6. O. C. Zienkiewicz and J. Z. Zhu, "Error estimates and adaptive refinement for plate bending problems", *Int. J. Numer. Meth. Eng.*, **28**, 2839-2853 (1989).
7. O. C. Zienkiewicz and J. Z. Zhu, "The superconvergent patch recovery and a posteriori error estimates. Part 1: The recovery technique", *Int. J. Numer. Meth. Eng.*, **33**, 1331-1364 (1992).
8. O. C. Zienkiewicz and J. Z. Zhu, "The superconvergent patch recovery and a posteriori error estimates. Part 2: Error estimates and adaptivity", *Int. J. Numer. Meth. Eng.*, **33**, 1365-1382 (1992).